Bioresource Technology 101 (2010) 4499–4507

Contents lists available at ScienceDirect

Bioresource Technology

journal homepage: www.elsevier.com/locate/biortech

Using FTIR spectroscopy for rapid determination of lipid accumulation in response to nitrogen limitation in freshwater microalgae

Andrew P. Dean, David C. Sigee, Beatriz Estrada, Jon K. Pittman *

Faculty of Life Sciences, University of Manchester, Michael Smith Building, Oxford Road, Manchester M13 9PT, UK

ARTICLE INFO

Article history:
Received 16 October 2009
Received in revised form 10 January 2010
Accepted 14 January 2010
Available online 11 February 2010

Keywords:
Microalgae
Nitrogen limitation
Lipid biosynthesis
Fourier transform infrared spectroscopy
Biofuel

ABSTRACT

In this study Fourier transform infrared micro-spectroscopy (FTIR) was used to determine lipid and carbohydrate content over time in the freshwater microalgae *Chlamydomonas reinhardtii* and *Scenedesmus subspicatus* grown in batch culture in limiting concentrations of nitrogen (N). Both algae exhibited restricted cell division and increased cell size following N-limitation. FTIR spectra of cells in N-limited media showed increasing lipid:amide I and carbohydrate:amide I ratios over time. The use of lipid- and starch-staining dyes confirmed that the observed ratio changes were due to increased lipid and carbohydrate synthesis. These results demonstrate rapid metabolic responses of *C. reinhardtii* and *S. subspicatus* to changing nutrient availability, and indicate the efficiency of FTIR as a reliable method for high-throughput determination of lipid induction.

1. Introduction

Biofuel production from renewable sources is widely considered to be one of the most sustainable alternatives to fossil fuels and a viable means to combat the environmental impact of fossil fuels on global warming (Hill et al., 2006). Microalgae have long been proposed as a potential renewable fuel source (Benemann et al., 1977; Oswald and Golueke, 1960) and extensive research funded by the US Department of Energy between 1978 and 1996 clearly validated this potential of microalgae (Sheehan et al., 1998). Microalgae are of particular interest as a sustainable source of biodiesel due to their ability to synthesise and accumulate significant quantities of lipids – up to approximately 80% of cell dry weight in some species (Chisti, 2007; Griffiths and Harrison, 2009; Sheehan et al., 1998). Under ideal growth conditions, many algal species produce saturated and unsaturated fatty acids which have potential nutritional value but are less ideal for biofuels, however, the synthesis of neutral lipids in the form of triacylglycerol can be induced in many species, for example under stress conditions, and these lipids are suitable precursors for biodiesel production (Hu et al., 2008; Miao and Wu, 2006).

Previous studies have demonstrated that nutrient stress conditions, such as nitrogen (N) starvation, phosphorus (P) starvation, urea limitation, and iron supplementation, can induce significant increases in lipid content in many microalgae species (Converti et al., 2009; Hsieh and Wu, 2009; Illman et al., 2000; Li et al., 2008; Liu et al., 2008; Pruvost et al., 2009; Rodolfi et al., 2009; Takagi et al., 2000; Tornabene et al., 1983). Commonly a 2- to 4-fold increase in lipid content has been observed in N-starved freshwater or marine microalgae such as in *Chlorella* and *Nannochloropsis* species (Illman et al., 2000; Rodolfi et al., 2009). Such studies therefore provide insights into the means by which mass culture conditions may be manipulated to increase oil production for biofuel applications. Despite significant lipid accumulation, microalgal biomass during nutrient stress is often reduced compared to cells grown under non-stressed conditions. A key aim of the algal biofuel research field is therefore to identify strains and mass culture conditions that provide high lipid yield coupled with high biomass productivity, and therefore increase overall lipid productivity.

Increasingly efficient and rapid methods of lipid detection are desirable. Methods of lipid detection include chromatographic-based separation and quantification of lipid classes (Krank et al., 2007) that require solvent extraction and fractionation but which are time-consuming. Another frequently used method makes use of the neutral lipid-staining fluorescent dye Nile Red. Nile Red can be used to image neutral lipid accumulation within cells or to quantify lipid biosynthesis by fluorescence spectroscopy (Cooksey et al., 1987; Elsey et al., 2007). However, Nile Red-based methods can also be time-consuming, are not as quantitative as chromatographic methods, and there may be variation in the efficiency of Nile Red accumulation into some algal species. An alternative approach is the use of Fourier transform infrared (FTIR) micro-spectroscopy. This is a method for whole organism analysis using intact cells which involves the measurement of infrared absorption in relation to a range of molecular vibrational modes

* Corresponding author. Tel.: +44 161 275 5235; fax: +44 161 275 5082.
E-mail address: jon.pittman@manchester.ac.uk (J.K. Pittman).

0960-8524/$ - see front matter © 2010 Elsevier Ltd. All rights reserved.
doi:10.1016/j.biortech.2010.01.065

(Murdock and Wetzel, 2009). Specific molecular groups can be identified by their absorption bands, allowing macromolecules (including proteins, lipids, carbohydrates, and nucleic acids) to be quantified.

A few studies have begun to demonstrate the potential of FTIR as a tool to identify changes in cellular components, including lipids, in response to a nutrient stress, such as low-N (Giordano et al., 2001; Heraud et al., 2005; Stehfest et al., 2005) and low-P (Dean et al., 2008; Sigee et al., 2007). In this study, we have used FTIR to investigate the effects of N-limitation on *Chlamydomonas reinhardtii* and *Scenedesmus subspicatus* grown in batch culture. We have examined how these microalgae species increase lipid and carbohydrate content following two different N-limitation stress treatments, and have validated the effectiveness of FTIR as an efficient method for determining lipid induction by comparison with the Nile Red method. Furthermore, this FTIR study extends on earlier observations of N-stressed algae (Giordano et al., 2001; Stehfest et al., 2005) by analysing the molecular response to N-availability with changes in growth phase during the batch culture cycle.

2. Methods

2.1. Cell cultivation

C. reinhardtii (CCAP 11/32A) and *S. subspicatus* (CCAP 276/20) were obtained from the Culture Collection of Algae and Protozoa, UK. Prior to the main experiment, algae were cultured in Jaworski's Medium (JM) to log phase, then filtered through a 1 μm filter membrane, washed in deionised water (to remove excess culture medium) and re-suspended in deionised water. An algal inoculum of 2 ml was then added to the experimental culture vessels (250 ml conical flasks) containing 200 ml of culture medium. The starting cell density was the same in all three treatments; 0.024×10^6 cells ml^{-1} for *C. reinhardtii*, and 0.18×10^6 cells ml^{-1} for *S. subspicatus*. The culture media consisted of unmodified JM with N (as NO_3) at concentrations of 19.6 mg l^{-1} (high-N culture) and modified JM, with N at concentrations of 3.0 mg l^{-1} (intermediate-N) and 0.8 mg l^{-1} (low-N). Each treatment consisted of triplicate flasks. Cultures were grown under a 16 h:8 h light dark cycle, at 25 °C, at a photon flux of approximately 150 μmol m^{-2} s^{-1}, on a orbital shaker at 120 rpm.

Cells were also grown in P limited media as a positive control, in order to validate the Nile Red staining (see below) of lipids. The culture media consisted of unmodified JM with P (as PO_4) at concentrations of 5.9 mg l^{-1} (high-P) and modified JM with P at concentrations of 0.05 mg l^{-1} (low-P). All other conditions were as described above.

2.2. Cell growth, nutrient, chlorophyll content, and protein analysis

Samples of cells and culture media were taken from the replicate flasks at regular intervals throughout the experiment. For cell counts, 1 ml of each algal culture was removed and preserved with 100 μl of Lugols' iodine prior to counting using a Sedgwick rafter slide and light microscope. For chlorophyll-a and nutrient analysis 5 ml of sample was filtered through a Whatman 0.45 μm cellulose acetate filter, with the deposit analysed for chlorophyll-a and the filtrate for NO_3–N and PO_4–P quantification. Chlorophyll-a was determined as described by Jespersen and Christoffersen (1987) following ethanol extraction. NO_3–N and PO_4–P in the culture media were analysed on a Skalar Sans Plus autoanalyser using standard methodology (Skalar Analytical). Cell volume was calculated by approximating the cells to a prolate spheroid for *S. subspicatus* and to a sphere for *C. reinhardtii* using the formulae given by Hillebrand et al. (1999). Total protein content was determined by Bradford assay following protein extraction by resuspending a frozen cell pellet in lysis buffer (50 mM Tris–HCl pH 8.0, 2% SDS, 10 mM EDTA, Sigma protease inhibitor mix) and performing three freeze–thaw cycles then incubating the cells for a further 1 h at room temperature before centrifugation at 13,000*g* for 20 min at 4 °C to remove cell debris.

2.3. FTIR spectroscopy

For FTIR spectroscopy a 0.5 ml sample was taken from each replicate flask for each treatment, mixed, centrifuged, the supernatant removed and the cells re-suspended in approximately 100 μm of distilled water 30 μl of which was then deposited on an 96 well silicon microplate, and oven-dried at 40 °C for 30 min. The plate was placed in a HTS-XT high-throughput microplate extension and FTIR spectra collected using a Bruker equinox 55 FTIR spectrometer, equipped with a mercury–cadmium–telluride detector cooled with liquid N_2. Spectra were collected over the wavenumber range 4000–600 cm^{-1}. Each sample was analysed in triplicate. Spectra were baseline corrected using the automatic baseline correction algorithm and were scaled to amide I. Principal component analysis (PCA) was performed using MATLAB.

2.4. Fluorescence microscopy and quantification

Neutral lipid-staining using Nile Red was performed essentially as described previously (Cooksey et al., 1987; Elsey et al., 2007). Cells were stained with 0.25 μg ml^{-1} Nile Red (9-diethylamino-5H-benzo[α]phenoxazine-5-one) (Invitrogen) solution in acetone and imaged by epi-fluorescence microscopy with a Leica DMR microscope using a 490 nm excitation/530 nm emission wavelength filter cube (Leica Microsystems). To obtain images of Nile Red fluorescence in conjunction with chlorophyll autofluorescence, Nile Red-stained cells were imaged using a broad-range UV excitation filter cube (340–380 nm excitation/>425 nm emission wavelength; Leica Microsystems). For starch-staining, cells were stained with Safranin O (Klut et al., 1989). Cells were stained with 0.02% Safranin O (Sigma) and were imaged by epi-fluorescence microscopy using a 436 nm excitation/480 nm emission wavelength filter cube (Chroma Technology). Relative fluorescence intensity of Nile Red and Safranin O staining was quantified on a fluorescence spectrometer (Jasco FP750) using 530 nm excitation and 575 nm emission (Nile Red), and 435 nm excitation and 480 nm emission wavelengths (Safranin O).

3. Results and discussion

3.1. Impact of N-limitation on algae biomass

The impact of N-limitation was examined on two biomass indicators, cell density and cell size. *C. reinhardtii* and *S. subspicatus* cells were grown in batch culture under N-replete and two N limiting conditions – an intermediate-N (3 mg l^{-1}) and low-N (0.8 mg l^{-1}) treatment. The high-N treatment (19.6 mg l^{-1}) was typical of a high-nutrient growth medium, in this case JM, and served as a reference for comparison with the N limiting experiments.

3.1.1. Cell density analysis

In all N treatments *C. reinhardtii* and *S. subspicatus* cell growth occurred with no distinctive lag phase but growth increased rapidly for the high-N treatments (Fig. 1a and b). All *C. reinhardtii* treatments entered stationary phase at the same time (day 21) although with significantly different cell counts, with the high-N

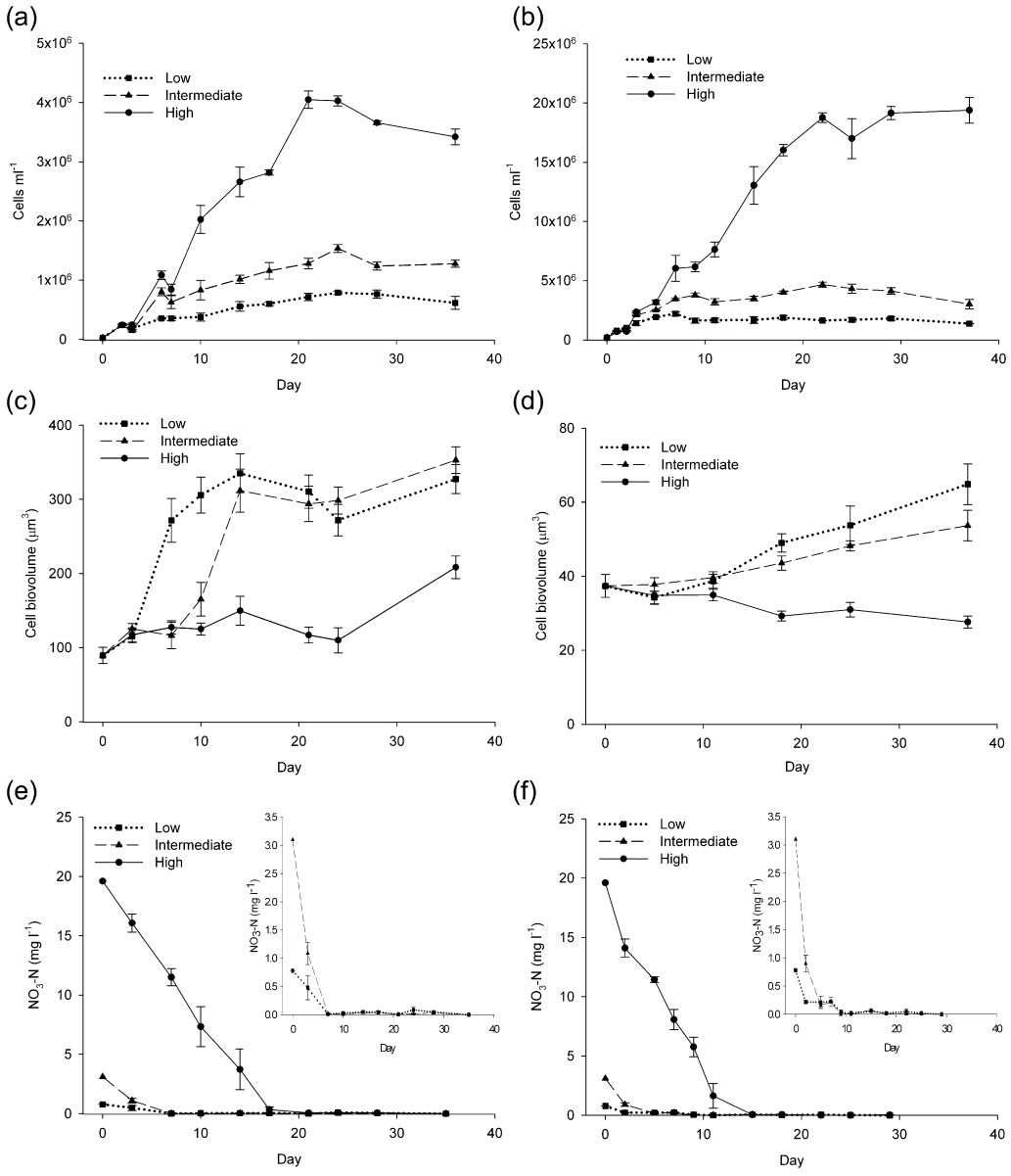

Fig. 1. Cell growth in response to varying N concentrations. Cell counts of *C. reinhardtii* (a) and *S. subspicatus* (b) cultures were compared to changes in mean single cell volume of *C. reinhardtii* (c) and *S. subspicatus* (d). Changes in N concentration within the culture media during the growth of *C. reinhardtii* (e) and *S. subspicatus* (f) in response to the varying N concentrations. Inset figures show the low and intermediate-N treatments in more detail. For all data sets, each point represents the mean (±SE) of three replicate culture flasks.

treatment reaching by far the highest cell count, entering stationary phase with a maximum of 4.1×10^6 cells ml^{-1}. *C. reinhardtii* cell counts were much lower in the intermediate- and low-N treatments, with the low-N treatment having the most reduced cell growth (Fig. 1a). Growth of *S. subspicatus* in the high-N treatment was also substantially greater than in the other two, with an exponential phase that lasted until day 22 and a final stationary phase population count of 18.8×10^6 cells ml^{-1} (Fig. 1b). The intermediate-N treatment also showed a gradual increase in population count to day 22. In the low-N treatment *S. subspicatus* cell counts showed no increase after day 7.

3.1.2. Cell volume analysis

For *C. reinhardtii*, the initial cell volume in all treatments was 89.3 ± 10.9 μm^3 per cell. The high-N treatment cells showed the least change in volume, with a minor increase by day 3 but with no further increase until late in the stationary phase (day 36) when volume increased to 208.4 ± 15.4 μm^3 (Fig. 1c). In contrast, in both the low- and intermediate-N treatments large cell volume increases were observed soon after the transfer of the stock culture into the experimental flasks. In the low-N treatment cells increased rapidly to reach 271.5 ± 29.5 μm^3 per cell by day 7, and reached a maximum on day 14. In the intermediate-N treatment the increase occurred slightly later, with a rapid increase between days 7 and 14 when volume increased from 116.3 ± 17.9 μm^3 to 311.8 ± 29.0 μm^3, and remained similar to those observed in the low-N treatment (Fig. 1c). *S. subspicatus* cell volume also showed distinct trends in relation to N-availability, with the high-N treatment decreasing in cell size from an initial value of 37.4 ± 3.1 μm^3–27.6 ± 1.7 μm^3 per cell (Fig. 1d). In contrast, low- and intermediate-N treatments each showed minor increases in cell size by the end of the growth period.

A number of previous studies have shown that N-limitation leads to an increase in individual cell volume, including in

C. reinhardtii (Van Donk et al., 1997) and *S. subspicatus* (Sterner et al., 1993). In contrast, other algae including *Ankistrodesmus* and *Stephanodiscus* have previously been shown to respond to N-limitation with a decrease in cell volume (Kilham et al., 1997; Lynn et al., 2000). We also found that both *C. reinhardtii* and *S. subspicatus* increased cell volume in response to N-limitation although the two algae differed in the magnitude of the cell volume increase; over 300% in *C. reinhardtii* but only about 50% in *S. subspicatus* (Fig. 1). Despite this significant increase in *C. reinhardtii* cell volume, the reduction in cell density following N-limitation meant that compared to the high-N culture biomass, the total biomass for the N-limited cultures was reduced. For example, by day 21 the intermediate-N culture biomass was reduced by 20.5%, and the low-N culture biomass was reduced by 53.1%. For *S. subspicatus*, as the significant reduction in cell density following N-limitation was coupled to only a very minor increase in cell volume, the intermediate-N total culture biomass was reduced by 61.4% compared to the high-N culture biomass and the low-N biomass was reduced by 84.9%.

3.2. Changes in nutrient accumulation in response to N-limitation

To confirm that the cells were accumulating N and to assess the accumulation of another macronutrient P, the concentration of these nutrients in the culture medium was measured over the duration of the growth assay. For both *C. reinhardtii* and *S. subspicatus* the rapid increase in cell density resulted in a rapid decrease in N (NO_3) in the culture medium (Fig. 1e and f). For all three N treatments the final concentration of NO_3 in the medium was undetectable (<0.01 mg l^{-1}). In the high-N treatment N concentrations fell to ~0.05 mg l^{-1} when the cells entered stationary phase. As the N concentrations were much lower in the low- and intermediate-N treatment media, N levels were depleted much more quickly, by day 7 for the *C. reinhardtii* cells and by day 9 for the *S. subspicatus* cells. In both treatments concentrations remained at or below 0.01 mg l^{-1} thereafter. In contrast, P (PO_4) concentration was not completely depleted in any of the treatments (Table 1) and always exceeded the critical P:N Redfield (mass) ratio of 1:7. This indicated that the culture media was N-limited but not P limited. However, P concentration did reduce over the course of the experiment, indicating that all cells were accumulating P. *C. reinhardtii* and *S. subspicatus* cells grown in the high-N media lead to a rapid decline in P content in the media, from approximately 7 mg l^{-1} at day 0 to below 1 mg l^{-1} by days 15–17. In contrast, P concentration reduced to a lesser extent in the media of the intermediate-N grown cells and to an even lesser extent in the media of the low-N grown cells, where P concentration was still above 3 mg l^{-1} by the end of the growth period (Table 1), due to a reduced amount of cells to accumulate P in these treatments. The rapid exhaustion of the N content in the media in the intermediate- and low-N treatments of both species demonstrated that these cells quickly became N-starved. This correlated with the exhibited physiological signs of N starvation observed within the first 3–5 days of growth, including reduced cell density, increased cell volume (Fig. 1), and decreased cellular chlorophyll-a (Table 2). In the high-N treated cells, similar signs of N deficiency were also observed, although only in stationary phase, correlating with complete depletion of external N supply much later in the experiment.

3.3. Lipid and carbohydrate detection by FTIR spectroscopy

Previous studies have screened algae for strains that accumulate significant quantities of lipids or have evaluated growth conditions such as nutrient starvation that induce lipid biosynthesis, in particular the biosynthesis of triacylglycerols (reviewed in Chisti (2007); Griffiths and Harrison (2009); Hu et al. (2008)). Many of these studies have used either chromatography or the Nile Red fluorescent stain to analyse lipid accumulation, but all of these methods have some drawbacks either due to being overly time-consuming, technically challenging or have poor efficiency or sensitivity. We examined the use of FTIR as a sensitive and high-throughput means to assess carbon allocation changes, including

Table 1
Changes in P concentration within the culture media during the growth of *C. reinhardtii* and *S. subspicatus* in response to the varying N concentrations. Each data value represents the mean (±SE) of three replicate culture flasks.

Growth phase	PO_4–P concentration (mg l^{-1})					
	Chlamydomonas reinhardtii			*Scenedesmus subspicatus*		
	Low-N	Intermediate-N	High-N	Low-N	Intermediate-N	High-N
Early growth[a]	6.13 ± 0.37	6.00 ± 0.12	5.60 ± 0.36	6.73 ± 0.07	5.47 ± 0.35	4.97 ± 0.32
Mid growth[b]	5.16 ± 0.12	3.05 ± 0.04	0.53 ± 0.15	5.53 ± 0.18	4.47 ± 0.13	0.87 ± 0.07
Late growth[c]	3.71 ± 0.01	2.60 ± 0.10	0.53 ± 0.14	6.15 ± 0.02	4.46 ± 0.12	0.63 ± 0.07

[a] Day 3 for *C. reinhardtii* and day 2 for *S. subspicatus*.
[b] Day 17 for *C. reinhardtii* and day 15 for *S. subspicatus*.
[c] Day 36 for *C. reinhardtii*c and day 29 for *S. subspicatus*.

Table 2
Changes in chlorophyll-a content of *C. reinhardtii* and *S. subspicatus* in response to varying N concentrations. Each data value represents the mean (±SE) of three replicate culture flasks.

Growth phase	Chlorophyll-a concentration (pg $cell^{-1}$)					
	Chlamydomonas reinhardtii			*Scenedesmus subspicatus*		
	Low-N	Inter-mediate-N	High-N	Low-N	Inter-mediate-N	High-N
Early growth[a]	0.083 ± 0.042	2.560 ± 0.490	2.199 ± 0.051	0.098 ± 0.061	0.443 ± 0.070	0.617 ± 0.111
Mid growth[b]	0.000 ± 0.000	0.085 ± 0.085	0.725 ± 0.124	0.022 ± 0.009	0.018 ± 0.001	0.187 ± 0.023
Late growth[c]	0.000 ± 0.000	0.000 ± 0.000	0.298 ± 0.024	0.009 ± 0.005	0.008 ± 0.001	0.084 ± 0.013

[a] Day 3 for *C. reinhardtii*a and day 2 for *S. subspicatus*.
[b] Day 17 for *C. reinhardtii* and day 15 for *S. subspicatus*.
[c] Day 36 for *C. reinhardtii* and day 29 for *S. subspicatus*.

lipid accumulation in two species of algae in response to N-limitation.

FTIR spectra of *C. reinhardtii* cells showed nine distinct absorption bands over the wavenumber range 1900–800 cm^{-1} (Supplementary Fig. 1 online). This profile was equivalent for *S. subspicatus* (data not shown). The bands were assigned to specific molecular groups on the basis of biochemical standards and published studies, as described previously (Stehfest et al., 2005). Bands were attributed to υ(C=O) stretching of amides from proteins (amide I, ~1655 cm^{-1}); δ(N–H) bending of amides from proteins (amide II, ~1545 cm^{-1}); $\delta_{as}(CH_2)$ and $\delta_{as}(CH_3)$ bending of methyl from proteins (~1455 cm^{-1}); and $\delta_s(CH_2)$ and $\delta_s(CH_3)$ bending of methyl and υ_s (C–O) stretching of COO– groups (~1380 cm^{-1}) and υ_{as} (>P=O) stretching, associated with phosphorus compounds (~1260 cm^{-1}). Two bands were of particular interest, the band at 1740 cm^{-1} which was associated with υ(C=O) of ester groups, primarily from lipids and fatty acids, and the region from 1200–950 cm^{-1} associated with υ(C–O–C) stretching of polysaccharides.

Measurements of total protein concentration in the algae samples indicated that protein content showed minimal change in response to N-limitation. For example, after 7 days growth in low-N medium, *C. reinhardtii* cells had an 18% reduction in total protein and *S. subspicatus* cells had a 15% reduction in total protein, while in intermediate-N medium total protein in *C. reinhardtii* cells and *S. subspicatus* cells reduced by 11% and 9%, respectively. This is in contrast to the observations of some previous studies. Cellular total protein was significantly reduced in the marine diatom *Chaetoceros muellerii* following N starvation (Giordano et al., 2001). However, the *C. reinhardtii* and *S. subspicatus* cells in this study were not grown under completely N-free conditions but in N-limited culture media containing reduced concentration of N, which may explain the minimal reduction in total protein. Other studies have also shown that for some microalgae, such as *Chlorella emersonii* and *Chlorella protothecoides*, low-N treatment does not significantly reduce protein content (Illman et al., 2000) suggesting that the impact of N-limitation on cellular protein may also be species dependent.

Due to the minimal reduction in protein content in response to N-limitation, it was therefore decided that the amide I band was a suitable band to use for normalisation of the FTIR spectra and ratio determination. Comparison of spectra (wavenumber region 1800–950 cm^{-1}) across the entire *C. reinhardtii* and *S. subspicatus* culture periods showed marked differences between N-replete and N-deficient cultures (Supplementary Fig. 1 online). Relatively little change occurred over time under conditions of high-N availability, but in intermediate- and low-N cultures, the lipid and carbohydrate bands showed rapid and marked changes.

3.3.1. Lipid:amide ratio analysis

Relative lipid content was determined by calculating the ratio of the lipid (1740 cm^{-1}) band to the amide I band (Fig. 2). An increase in the lipid:amide ratio from an initial value of 0.2 occurred in all treatments in both species. In the *C. reinhardtii* cells grown in the high-N treatment, the lipid:amide band ratio was relatively unchanged by day 28 followed by a large increase to reach 1.0 on day 36 (Fig. 2a). The low- and intermediate-N treatments displayed much greater increases in their lipid:amide ratio and both reached a similar final intensity (~1.28), but with the increase in the low-N treatment occurring rapidly from day 3, while the increase in the intermediate-N treatment occurred from day 10. In the *S. subspicatus* cells the lipid:amide ratio rapidly increased from day 0 for the low-N culture and from day 5 for the intermediate-N culture and

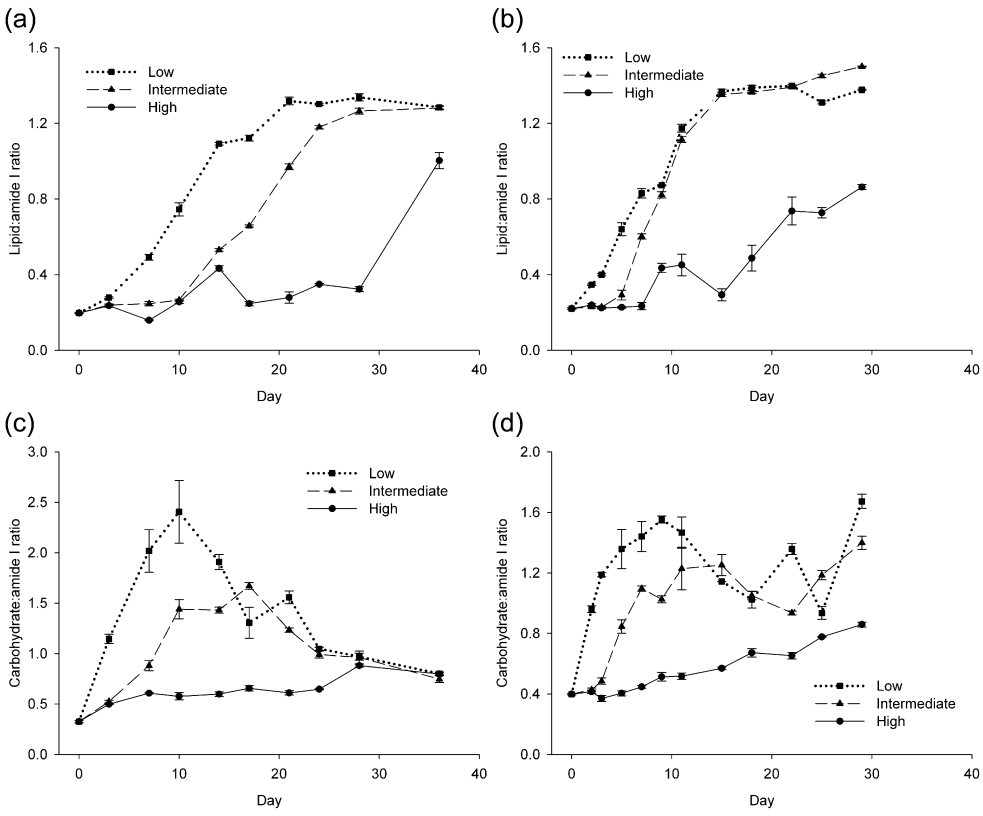

Fig. 2. Changes in the lipid:amide I ratio (a) and (b), and the carbohydrate:amide I ratio (c) and (d) within cells of *C. reinhardtii* (a) and (c), and *S. subspicatus* (b) and (d) in response to varying N concentrations. For all data sets, each point is the mean (±SE) of three FTIR spectra from pooled samples (derived from three replicate flasks). Each of the spectra was separately derived from randomly selected small groups of cells within the oven-dried preparation.

reached a ratio of ~1.4 by day 15. The lipid:amide ratio reached a plateau in both N-limited algae, suggesting that there may be a limit to the amount of lipid that the cells can synthesise in response to N-limitation. Cells grown in the high-N cultures showed a much slower rate of increase, reaching a ratio of 0.86 on day 29 (Fig. 2b). This increase occurred only during stationary phase as the high-N treated cells became progressively more N-deficient.

A number of earlier examinations of nutrient stress-induced lipid induction assessed N starvation alone with growth in medium containing very low concentrations of N (e.g. Tornabene et al., 1983). As shown in previous studies and in this study, N starvation significantly inhibits cell growth and total biomass, and thus despite significant lipid biosynthesis the cell biomass in N-starved cultures is often too low for efficient biodiesel production. For example, the lipid productivity of the *S. subspicatus* culture, as indicated by lipid content per unit biomass, was lowest in the low-N treated culture. At day 21 *S. subspicatus* lipid productivity was reduced slightly in the intermediate-N culture compared to the high-N culture and reduced markedly in the low-N culture by over 50%. Inhibition of cell growth was less marked in the intermediate-N treatments compared to the low-N treatments but significant lipid induction, as indicated by high lipid:amide ratios, was maintained for both treatments, particularly for *S. subspicatus* where the lipid:amide ratios after day 10 were essentially identical between low-N and intermediate-N treatments (Fig. 2b). This led to an increase in lipid productivity in the intermediate-N treatments compared to the high-N treatments. This was particularly clear for the *C. reinhardtii* intermediate-N cultures which had 30–40% greater lipid productivity than the high-N cultures at days 14 and 21. These experiments therefore indicate that optimisation of nutrient limitation conditions rather than complete starvation offers the potential to increase lipid productivity. Other studies have indicated similar potential. For example, *Neochloris oleobundans* grown in 5 mM sodium nitrate provides slightly greater lipid productivity compared to cells grown in 3 mM sodium nitrate medium (Li et al., 2008). However, a recent study of *Chlorella vulgaris* found no significant difference in the lipid productivity of the algae grown in a low-N growth medium compared to an intermediate-N medium (Converti et al., 2009). Optimisation of nutrient limitation conditions may therefore not be useful for all species. It has been argued that biomass productivity more so than lipid content is a critical determinant of lipid productivity (Griffiths and Harrison, 2009), therefore if species can be identified which respond to optimised nutrient limitation by preventing significant reduction in culture biomass, lipid productivity may be significantly enhanced.

3.3.2. Carbohydrate:amide ratio analysis

Relative carbohydrate content was determined by calculating the ratio of the carbohydrate (1200–950 cm^{-1}) bands to the amide I band. The ratio of carbohydrate to amide showed a gradual increase in the high-N treatment of both *C. reinhardtii* and *S. subspicatus*, increasing from an initial value of 0.3–0.4 to a final value of ~0.80 (Fig. 2c and d). However, in both the intermediate- and low-N treatments the ratio showed a rapid increase until day 10 followed by a subsequent decline, but with a much faster rate of increase in the low-N cultures. This pattern was equivalent in *C. reinhardtii* and *S. subspicatus* although the overall values differed with a maximal carbohydrate:amide ratio of 2.41 in the low-N *C. reinhardtii* cells and a maximal ratio of 1.55 in the low-N *S. subspicatus* cells (Fig. 2c and d). The decline in carbohydrate:amide ratio in the low- and intermediate-N treatments was more marked in *C. reinhardtii* and the final ratio was the same in all three treatments. This suggests that after an initial increase in the synthesis of carbohydrate it was then utilised as the cells reached stationary phase. In contrast, in the *S. subspicatus* low- and intermediate-N treated cells there were only minor declines in carbohydrate:amide ratio and a further increase on the final sampling day (day 29), up to 1.4 for the intermediate-N treatment and up to 1.67 for the low-N treatment (Fig. 2d). Generally, in all low- and intermediate-N treatments, the increase in the carbohydrate:amide ratio occurred earlier than the increase in lipid:amide ratio.

3.3.3. Principal component analysis

In addition to calculating lipid:amide and carbohydrate:amide ratios, multivariate analysis was used. The 1800–950 cm^{-1} range FTIR spectra for each sample day were further analysed by principal component analysis (PCA) to determine to which extent the separate treatments could be differentiated. PCA clearly resolved the data into two major components for both species. For *C. reinhardtii* PC1 accounted for 61% of the variation and PC2 for 35%, while for *S. subspicatus* PC1 accounted for 81% of the variation and PC2 for 15%. PC scores plots of PC1 against PC2 were generated for the FTIR spectra from *C. reinhardtii* (Fig. 3a) and *S. subspicatus* (Fig. 3b) for each sample day. The plots show a clear separation of the high-N treatments from the intermediate- and low-N treatments for both species, indicating that the carbon metabolism

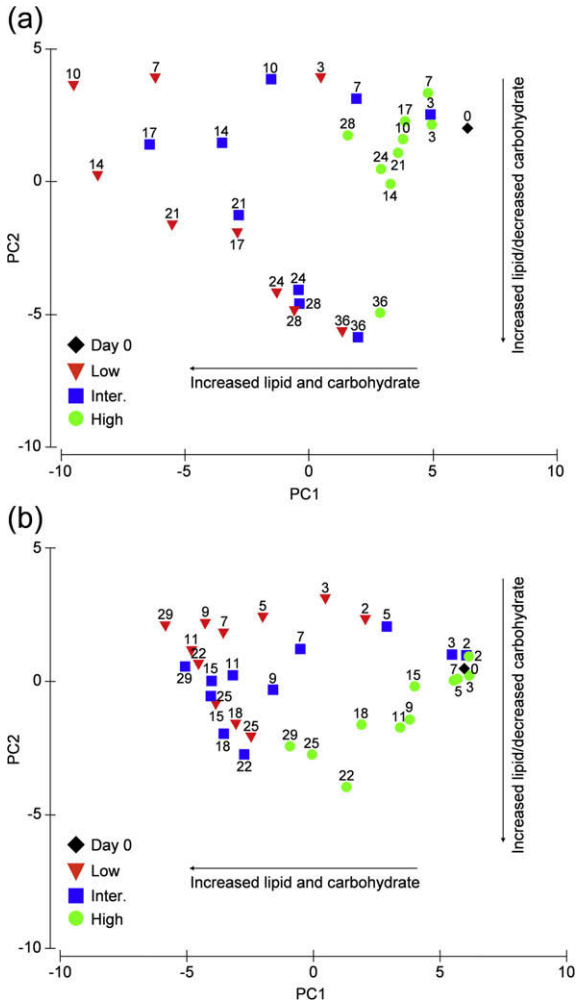

Fig. 3. Principal component analysis (PCA) of FTIR spectra derived from cells of *C. reinhardtii* (a) and *S. subspicatus* (b) in response to varying N concentrations. PCA was performed using the spectral range 1800–950 cm^{-1} on baseline corrected spectra normalised to amide I. Scores plots for principle components (PC) 1 and 2 are shown. Spectra of cells from high-N, intermediate-N and low-N are represented by the indicated symbols. The number next to each symbol indicates the day of growth.

changes were closely similar for both N-limited treatments, but less separation between the intermediate- and low-N treatments. By comparing the PCA scores over the duration of the batch growth and analysing the PC loading plots, PCA was able to clearly differentiate between the initial and latter phases of N-limited growth. The *C. reinhardtii* plots indicate that the low-N treatments for the first 10 days, and the intermediate-N treatments for the first 17 days, only change significantly with respect to PC1 and not PC2, then for the later sampling days the variation is with respect predominantly to PC2 (Fig. 3a). The *S. subspicatus* plots show an equivalent trend although the variation between days is not as marked (Fig. 3b). The PC loadings indicate that along PC1 the main variation occurs within the lipid and carbohydrate regions, with an increased negative loading indicating increasing lipid and carbohydrate accumulation, while along PC2 the main variation also occurs within the lipid and carbohydrate regions but with the increased negative loadings indicating increasing lipid but decreasing carbohydrate accumulation (data not shown). Thus the PCA identified that both lipid and carbohydrate increase in the initial phase of growth, followed by continued lipid increase but a decrease in carbohydrate content. PCA of FTIR spectra was therefore as effective in determining the relative increases in lipid content as calculating the peak height ratios of specific bands. Furthermore, such multivariate analysis is much faster to perform than individual band analysis and is therefore a more efficient and potentially high-throughput means for FTIR analysis.

3.3.4. Cell volume changes in relation to lipid and carbohydrate content

In N-limited *C. reinhardtii*, the increase in the lipid content identified by FTIR correlated with the increase in cell size (at day 0 in the low-N treatment, at day 7 in the intermediate-N treatment) (Fig. 1c) indicating that the cell volume changes are due to an increase in the synthesis and storage of lipid. The increased cell size also corresponded to the initial increase in the carbohydrate content, however, there was no decrease in the cell volume when the carbohydrate levels subsequently decreased, and no correlation between carbohydrate and cell volume was observed. This would suggest that the primary cause of increased cell volume is increased lipid synthesis and the accumulation of lipid bodies which were clearly observed in the cells (Supplementary Fig. 2 online). In *S. subspicatus* the relationship between cell volume, lipid and carbohydrate synthesis was different. Under N-limited conditions the carbohydrate content and cell volume showed no correlation while the lipid content was only weakly correlated with cell volume. The rapid increase in lipid abundance (Fig. 2b) was not reflected in cell volume which showed a gentle increase throughout the growth phase (Fig. 1d). This is similar to a previous

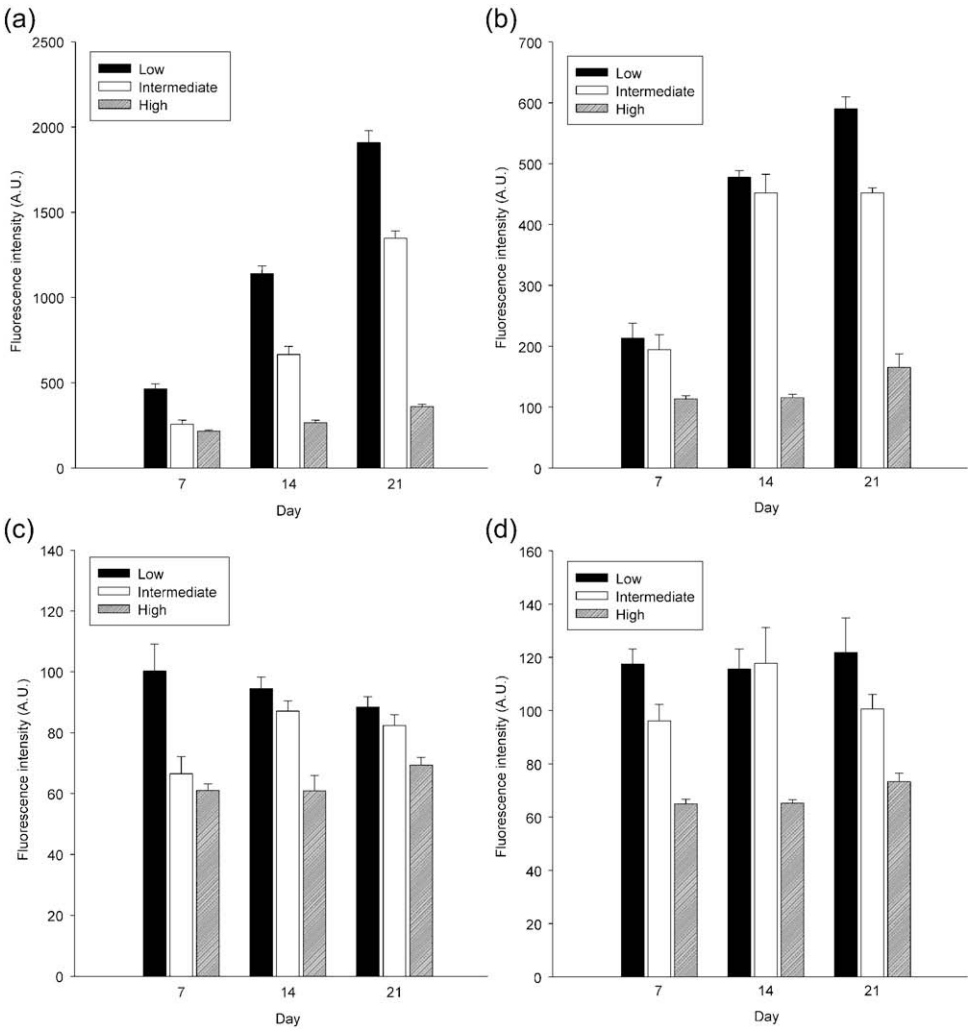

Fig. 4. Relative neutral lipid content (a) and (b), and starch content (c) and (d) within Nile Red- and Safranin O-stained cells of *C. reinhardtii* (a) and (c), and *S. subspicatus* (b) and (d) in response to varying N concentrations. For each treatment and time point the fluorescence emission of Nile Red (lipid) and Safranin O (starch) were quantified from 5×10^5 cells per sample. Each data point is a mean (±SE) of six samples.

analysis of *S. subspicatus* response to P limitation where increased lipid and carbohydrate accumulation was not associated with increased cell volume (Sigee et al., 2007).

3.4. Fluorescence detection of lipid and carbohydrate accumulation

The lipid and carbohydrate accumulation in the *C. reinhardtii* and *S. subspicatus* cells in response to limiting N was inferred by the lipid:amide and carbohydrate:amide ratios derived from the FTIR spectra. To validate the effectiveness of FTIR as a high-throughput determination method of lipid and biomass, neutral lipid accumulation in the cells was confirmed by the Nile Red method (Cooksey et al., 1987; Elsey et al., 2007) and starch accumulation (as an indicator for carbohydrate accumulation) was confirmed using the starch-staining fluorescence dye Safranin O (Klut et al., 1989). *C. reinhardtii* cells grown under the low-N treatment showed significant accumulation of lipid bodies which stained positive for neutral lipids by Nile Red while the high-N treated cells accumulated no neutral lipids (Supplementary Fig. 2 online). Nile Red staining was harder to visualise in *S. subspicatus* particularly due to the smaller size of the cells, however, increased accumulation of lipid bodies in these cells following nutrient limitation was similarly observed (Supplementary Fig. 2 online). Starch accumulation was observed in the low-N treated cells by Safranin O staining. Quantification of the Nile Red fluorescence (Fig. 4a and b) and the Safranin O fluorescence (Fig. 4c and d) confirmed the significant induction of neutral lipids and starch following limiting N treatment in *C. reinhardtii* and *S. subspicatus* over time. Both Nile Red and Safranin O detected the same relative accumulation in lipids and carbohydrates in response to N-limitation as indicated by FTIR in both species. Correlation analysis was performed between the FTIR lipid:amide and Nile Red fluorescence data, and the FTIR carbohydrate:amide and Safranin O fluorescence data from *C. reinhardtii* and *S. subspicatus*. Very strong correlation was determined between the FTIR- and Nile Red-based lipid measurements (coefficient of determination $r^2 = 0.9301$ for *C. reinhardtii* and $r^2 = 0.9002$ for *S. subspicatus*) (Supplementary Fig. 3 online). The correlation between the carbohydrate:amide data and the Safranin O-based starch measurements were also strong ($r^2 = 0.8358$ for *C. reinhardtii* and $r^2 = 0.9296$ for *S. subspicatus*). These strong correlations thus validate the FTIR technique as an effective method for lipid and carbohydrate determination in these algae. This correlation data also confirms that the observed lipid:amide and carbohydrate:amide ratio increases were not caused by a decrease in cellular protein concentration and suggests that the amide I band can be a suitable marker for FTIR spectra normalisation in some situations.

Previous studies on the effect of another nutrient limitation stress, P limitation, used FTIR to infer the cellular accumulation of lipid in *C. reinhardtii* and *S. subspicatus* (Dean et al., 2008; Sigee et al., 2007). Nile Red staining further confirmed the induction of lipid accumulation in response to P limitation in these species (Supplementary Fig. 2 online), thus also validating the effectiveness of FTIR as a means to measure lipid accumulation in response to a variety of stresses. Although these analyses demonstrate that FTIR and Nile Red are equally effective at measuring lipid accumulation, FTIR is likely to be a more efficient tool for this purpose due to much faster analysis time and high reproducibility of results (Murdock and Wetzel, 2009). Furthermore, FTIR allows for the simultaneous analysis of multiple metabolites which will allow more detailed monitoring of the biofuel feedstock culture if necessary. FTIR may also be more suitable than Nile Red for efficiently detecting large increases in lipid concentration. Nile Red does not appear to be efficient at accurately quantifying lipid concentration above 20 μg/ml (Chen et al., 2009) while FTIR can efficiently detect linear lipid concentration changes up to at least 250 μg (Dreissig et al., 2009).

4. Conclusions

This study has shown that *C. reinhardtii* and *S. subspicatus* can elicit rapid and distinctive changes in cellular carbon allocation with growth stage and nutrient availability. These microalgae are therefore able to adapt rapidly to transient changes in nutrient availability within the environment. These studies have also demonstrated that FTIR analysis can effectively identify changes in lipid and carbohydrate content in algal cells in response to an induction treatment. This demonstrates that FTIR will be an efficient tool for rapidly monitoring lipid accumulation of microalgae at multiple stages of growth following lipid induction, and will therefore have applications for algal biofuel production processes.

Acknowledgements

This work was funded in part by financial support from The Leverhulme Trust (Grant No. F/00 120/AO to D.C.S. and F/00 120/BG to J.K.P.). J.K.P. is a grateful recipient of a BBSRC David Phillips Fellowship.

Appendix A. Supplementary data

Supplementary data associated with this article can be found, in the online version, at doi:10.1016/j.biortech.2010.01.065.

References

Benemann, J.R., Weissman, J.C., Koopman, B.L., Oswald, W.J., 1977. Energy production by microbial photosynthesis. Nature 268, 19–23.
Chen, W., Zhang, C.W., Song, L.R., Sommerfeld, M., Hu, Q., 2009. A high throughput Nile Red method for quantitative measurement of neutral lipids in microalgae. J. Microbiol. Methods 77, 41–47.
Chisti, Y., 2007. Biodiesel from microalgae. Biotechnol. Adv. 25, 294–306.
Converti, A., Casazza, A.A., Ortiz, E.Y., Perego, P., Del Borghi, M., 2009. Effect of temperature and nitrogen concentration on the growth and lipid content of *Nannochloropsis oculata* and *Chlorella vulgaris* for biodiesel production. Chem. Eng. Process. 48, 1146–1151.
Cooksey, K.E., Guckert, J.B., Williams, S.A., Callis, P.R., 1987. Fluorometric determination of the neutral lipid content of microalgal cells using Nile Red. J. Microbiol. Methods 6, 333–345.
Dean, A.P., Nicholson, J.M., Sigee, D.C., 2008. Impact of phosphorus quota and growth phase on carbon allocation in *Chlamydomonas reinhardtii*: an FTIR microspectroscopy study. Eur. J. Phycol. 43, 345–354.
Dreissig, I., Machill, S., Salzer, R., Krafft, C., 2009. Quantification of brain lipids by FTIR spectroscopy and partial least squares regression. Spectrochim. Acta A 71, 2069–2075.
Elsey, D., Jameson, D., Raleigh, B., Cooney, M.J., 2007. Fluorescent measurement of microalgal neutral lipids. J. Microbiol. Methods 68, 639–642.
Giordano, M., Kansiz, M., Heraud, P., Beardall, J., Wood, B., McNaughton, D., 2001. Fourier transform infrared spectroscopy as a novel tool to investigate changes in intracellular macromolecular pools in the marine microalga *Chaetoceros muellerii* (Bacillariophyceae). J. Phycol. 37, 271–279.
Griffiths, M.J., Harrison, S.T.L., 2009. Lipid productivity as a key characteristic for choosing algal species for biodiesel production. J. Appl. Phycol. 21, 493–507.
Heraud, P., Wood, B.R., Tobin, M.J., Beardall, J., McNaughton, D., 2005. Mapping of nutrient-induced biochemical changes in living algal cells using synchrotron infrared microspectroscopy. FEMS Microbiol. Lett. 249, 219–225.
Hill, J., Nelson, E., Tilman, D., Polasky, S., Tiffany, D., 2006. Environmental, economic, and energetic costs and benefits of biodiesel and ethanol biofuels. Proc. Natl. Acad. Sci. USA 103, 11206–11210.
Hillebrand, H., Durselen, C.D., Kirschtel, D., Pollingher, U., Zohary, T., 1999. Biovolume calculation for pelagic and benthic microalgae. J. Phycol. 35, 403–424.
Hsieh, C.H., Wu, W.T., 2009. Cultivation of microalgae for oil production with a cultivation strategy of urea limitation. Bioresour. Technol. 100, 3921–3926.
Hu, Q., Sommerfeld, M., Jarvis, E., Ghirardi, M., Posewitz, M., Seibert, M., Darzins, A., 2008. Microalgal triacylglycerols as feedstocks for biofuel production: perspectives and advances. Plant J. 54, 621–639.
Illman, A.M., Scragg, A.H., Shales, S.W., 2000. Increase in *Chlorella* strains calorific values when grown in low nitrogen medium. Enzyme Microb. Technol. 27, 631–635.
Jespersen, A., Christoffersen, K., 1987. Measurements of chlorophyll-a from phytoplankton using ethanol as extraction solvent. Arch. Hydrobiol. 109, 445–454.

Kilham, S.S., Kreeger, D.A., Goulden, C.E., Lynn, S.G., 1997. Effects of nutrient limitation on biochemical constituents of *Ankistrodesmus falcatus*. Freshwater Biol. 38, 591–596.

Klut, M.E., Stockner, J., Bisalputra, T., 1989. Further use of fluorochromes in the cytochemical characterization of phytoplankton. Histochem. J. 21, 645–650.

Krank, J., Murphy, R.C., Barkley, R.M., Duchoslav, E., McAnoy, A., 2007. Qualitative analysis and quantitative assessment of changes in neutral glycerol lipid molecular species within cells. Methods Enzymol. 432, 1–20.

Li, Y.Q., Horsman, M., Wang, B., Wu, N., Lan, C.Q., 2008. Effects of nitrogen sources on cell growth and lipid accumulation of green alga *Neochloris oleoabundans*. Appl. Microbiol. Biotechnol. 81, 629–636.

Liu, Z.Y., Wang, G.C., Zhou, B.C., 2008. Effect of iron on growth and lipid accumulation in *Chlorella vulgaris*. Bioresour. Technol. 99, 4717–4722.

Lynn, S.G., Kilham, S.S., Kreeger, D.A., Interlandi, S.J., 2000. Effect of nutrient availability on the biochemical and elemental stoichiometry in the freshwater diatom *Stephanodiscus minutulus* (Bacillariophyceae). J. Phycol. 36, 510–522.

Miao, X.L., Wu, Q.Y., 2006. Biodiesel production from heterotrophic microalgal oil. Bioresour. Technol. 97, 841–846.

Murdock, J.N., Wetzel, D.L., 2009. FT-IR microspectroscopy enhances biological and ecological analysis of algae. Appl. Spectrosc. Rev. 44, 335–361.

Oswald, W.J., Golueke, C.G., 1960. Biological transformation of solar energy. Adv. Appl. Microbiol. 2, 223–262.

Pruvost, J., Van Vooren, G., Cogne, G., Legrand, J., 2009. Investigation of biomass and lipids production with *Neochloris oleoabundans* in photobioreactor. Bioresour. Technol. 100, 5988–5995.

Rodolfi, L., Zittelli, G.C., Bassi, N., Padovani, G., Biondi, N., Bonini, G., Tredici, M.R., 2009. Microalgae for oil: strain selection, induction of lipid synthesis and outdoor mass cultivation in a low-cost photobioreactor. Biotechnol. Bioeng. 102, 100–112.

Sheehan, J., Dunahay, T., Benemann, J., Roessler, P., 1998. A Look Back at the US Department of Energy's Aquatic Species Program: Biodiesel from Algae. National Renewable Energy Laboratory, Report NREL/TP-580-24190.

Sigee, D.C., Bahram, F., Estrada, B., Webster, R.E., Dean, A.P., 2007. The influence of phosphorus availability on carbon allocation and P quota in *Scenedesmus subspicatus*: a synchrotron-based FTIR analysis. Phycologia 46, 583–592.

Stehfest, K., Toepel, J., Wilhelm, C., 2005. The application of micro-FTIR spectroscopy to analyze nutrient stress-related changes in biomass composition of phytoplankton algae. Plant Physiol. Biochem. 43, 717–726.

Sterner, R.W., Hagemeier, D.D., Smith, W.L., 1993. Phytoplankton nutrient limitation and food quality for Daphnia. Limnol. Oceanography 38, 857–871.

Takagi, M., Watanabe, K., Yamaberi, K., Yoshida, T., 2000. Limited feeding of potassium nitrate for intracellular lipid and triglyceride accumulation of *Nannochloris* sp. UTEX LB1999. Appl. Microbiol. Biotechnol. 54, 112–117.

Tornabene, T.G., Holzer, G., Lien, S., Burris, N., 1983. Lipid composition of the nitrogen starved green alga *Neochloris oleoabundans*. Enzyme Microb. Technol. 5, 435–440.

Van Donk, E., Lurling, M., Hessen, D.O., Lokhorst, G.M., 1997. Altered cell wall morphology in nutrient-deficient phytoplankton and its impact on grazers. Limnol. Oceanography 42, 357–364.